J. Phys. D: Appl. Phys. 27 (1994) 1038–1045. Printed in the UK

Electron field emission from large-area cathodes: evidence for the projection model

M Jimenez†, R J Noer†§, G Jouve†‖, J Jodet‡ and B Bonin†

† Commissariat à l'Energie Atomique, DSM/DAPNIA/SEA, Centre d'Etudes de Saclay, F-91191 Gif-sur-Yvette Cedex, France
‡ Commissariat à l'Energie Atomique, INSTN/SEPEM, Centre d'Etudes de Saclay, F-91191 Gif-sur-Yvette Cedex, France

Received 4 October 1993, in final form 1 January 1994

Abstract. Field emission from two special kinds of emitters has been studied in detail: intentionally introduced particles of controlled geometry, and sites produced by intentional mechanical damage to the cathode surface. We found that the size of particles seems to play no role in their threshold field but their shapes are a determinant factor since spherical particles do not emit for fields up to 120 MV m^{-1}. The method of creation of damage sites, and the similarity of their emission on Nb and Au substrates, suggest the possibility that emission comes from geometrical protrusions. A model of superposed geometrical protrusions is proposed to explain the enhanced field emission behaviour of this particular type of surface defect.

1. Introduction

It is well known [1, 2] that the application of an electric field to cathodes of macroscopic size (such as 1 cm^2) brings about measurable emission of electrons from spatially localized sites at fields of the order of tens of megavolts per metre, roughly 100 times less than the fields necessary for the classic field emission originally described by Fowler and Nordheim [3]. For many years, this anomalous emission was universally explained by invoking a 'projection model'. This model assumes the presence on the cathode surface of one or more microscopic projections, sharp enough to cause a geometric enhancement of the local field at the projection tip to a value some 100 times greater than the nominally applied field.

More recently, however, this model has generally fallen from favour, being superseded by others that assume the involvement of insulating materials at the emission site [4]. Among the reasons for its downfall are

(i) the failure to observe, with modern scanning electron microscopes of increasingly high resolution, any projections of sufficient sharpness to account for the anomalously low threshold fields for emission,

(ii) the frequent SEM observation of what appears to be insulating particles or inclusions in conjunction with emission sites, and

(iii) the observation of features in the energy spectrum of both electrons [5] and light [6] emitted by such sites that are not predicted by the projection model but are plausibly in accord with the involvement of insulators or semiconductors.

Our recent study of electron emission from cathodes contaminated with intentionally introduced particles of known composition [7], however, resulted in three kinds of surprising observations that suggest anew the applicability of a simple projection model. The first of these is the low threshold field for emission from particles of gold placed on a clean gold substrate; here the interface between particle and substrate is expected to be metallic, with no involvement of insulators. The second concerns instances where evidence of melting was found at the interface between iron particles and the Nb substrate on which they had been placed, after these particles had been observed to emit strongly. It would seem unlikely that such a molten interface could retain any insulating character. The third is the observation that Fe particles, placed on a Nb substrate covered with a thick (240 nm) and initially insulating oxide layer, lost their ability to retain electric charge once they had been observed to emit; that is, once again, the particle/substrate interface appears to be conducting.

In this paper we report more recent measurements that we have carried out, designed to test the applicability

§ On leave of absence from Department of Physics, Carleton College, Northfield, Minnesota 55057, USA.

‖ On leave of absence from the Laboratoire de Métallurgie Structurale, Bâtiment 413, Université de Paris-Sud, F-91405 Orsay Cedex, France.

0022-3727/94/051038+08$19.50

of the projection model in two new ways. The first concerns emission from intentionally introduced particles of controlled geometry. The second concerns emission from sites produced by intentional mechanical damage to the cathode surface. In both cases we find, once again, that the emission behaviour is consistent with the projection model and difficult to explain by invoking the presence of insulators. We also present a simple theoretical idea and the results of some numerical calculations that suggest a way in which a projection much less sharp than those invoked in the past can produce the observed emission characteristics.

2. Apparatus and procedures

Our apparatus, consisting of a commercial SEM modified for field emission measurements by the addition of a tungsten scanning anode, is identical with that described in our previous paper [7], as are our basic measurement techniques. Our cathodes are Nb (electropolished) and Au (mechanically polished). Contaminant particles, introduced as potential emission sites, are initially anchored to the substrate with the aid of a layer of moisture (humidity). To measure the emission from a site, a flat anode (end radius 40 μm) is brought lightly into contact with the substrate a few tens of micrometres away from the site, raised a known distance d (typically 50 μm), and then centred above the site. The applied field is determined, to a good approximation, by $E = V/d$, where V is the potential applied to the anode. The threshold emission field is taken to be the field that produces the minimum detectable emission current above the background noise (typically several picoampères).

3. Results

3.1. Spherical and irregular particles

The first measurements that we report concern emission from Ni particles of varying geometry placed on substrates of Nb and Au. Nickel, like the iron we studied earlier, oxidizes in air with formation of a semiconducting oxide layer [8] of thickness about 1 nm [9, 10]. We studied Ni particles with two kinds of geometry: spherical and irregular (both obtained commercially). The size of the spherical particles is in the range 10–20 μm; that of the irregular particles is 5–10 μm. Figures 1(a) and (b) show a representative particle of each type. The emission observed from the irregular particles is shown in figure 2(a), and is similar to that observed earlier [7] with irregular particles of Fe: a wide spread of thresholds, with many falling in the range (below 50 MV m^{-1}) that we associate with 'good' emitters, and all emitting at fields less than the lower limits found previously [7] for two kinds of insulators (Al_2O_3 and SiO_2). The spherical particles, however, were completely different (figure 2(b)): with three

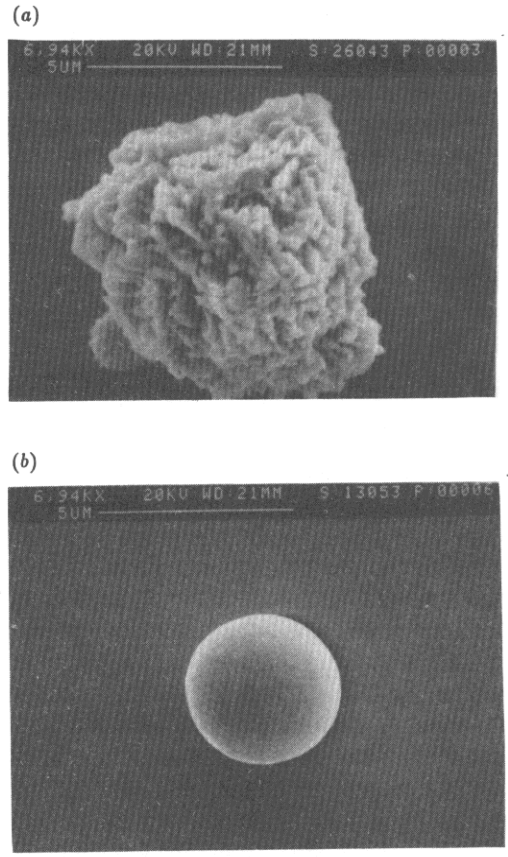

Figure 1. Nickel particles used as potential emission sites: (a) irregular, (b) spherical.

exceptions out of 30 particles measured, no emission was seen up to 120 MV m^{-1}. No significant differences were seen between Nb and Au substrates. The experiment was repeated with iron particles (both spherical and irregular) with similar results (figures 3(a) and (b)).

The studies of emission from irregular particles of various sizes (2–30 μm) did not show any relation between the particle size and its threshold field.

3.2. Mechanical damage sites

We have often observed that a scratch or indentation of a cathode surface (such as from accidental contact with an anode tip) will produce an emission site. It is easy to imagine how emission from such a site might result from a projection, and difficult to see how it could involve an insulator mechanism. Hence we thought a study of the emission from this kind of site might be fruitful in distinguishing between these alternative kinds of mechanism.

To produce mechanical damage on a cathode surface with the least chance of contamination, we used a diamond tool (a commercial phonograph stylus). A diamond stylus on its metal support was mounted in place of one of the three anodes that our apparatus can accommodate (see figure 4). Under SEM observation, the stylus was brought in contact with the substrate, and the anode arm was further lowered by several micrometres. This procedure results in a flexing of the stylus support and a slight lateral as well as vertical movement; when

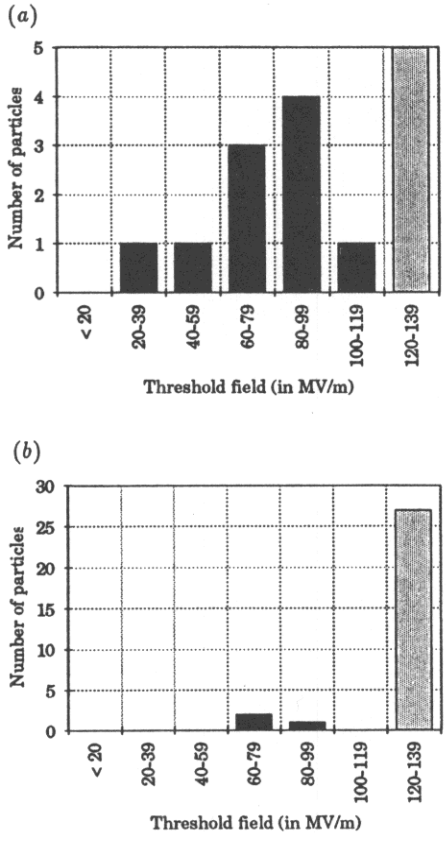

Figure 2. Emission tests for Ni particles on a Nb substrate. Dark bars show threshold fields for measured emission; light bars show the maximum field attained when no emission was seen: (*a*) irregular particles, (*b*) spherical particles.

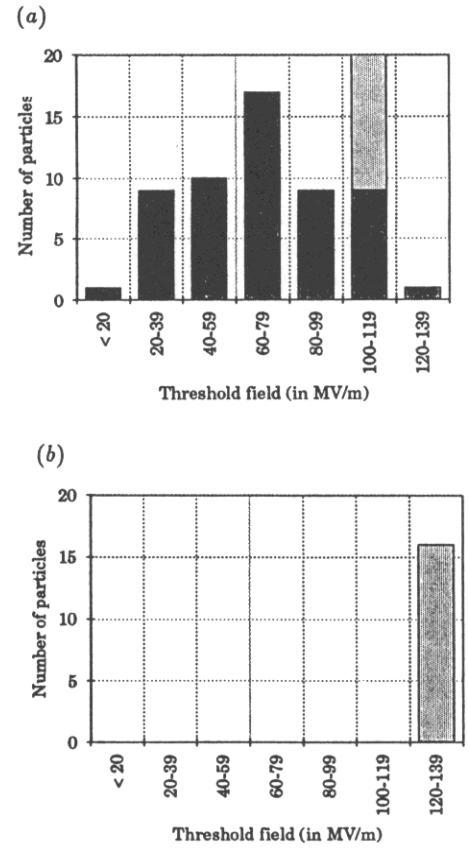

Figure 3. Emission tests for Fe particles on a Nb substrate. Dark bars show threshold fields for measured emission; light bars show maximum field attained when no emission was seen: (*a*) irregular particles, (*b*) spherical particles.

the anode arm is raised, a characteristic 'footprint' of the type shown in figure 5 (designated a 'point' defect) is evident. Alternatively, the substrate can be moved laterally (manually, in an irregular fashion) before the anode arm is raised, resulting in the kind of 'scratch' defect that is shown in figure 6.

Point defects were observed to be good emitters; figure 7 shows the statistics for such defects, each produced nominally in the same fashion. The results obtained on a Nb substrate (figure 7(*a*)) are similar to those obtained on a Au substrate (figure 7(*b*)). Scratch defects on Au and Nb substrates, when scanned with an anode, invariably show emission sites at those points along the scratch where substrate material, 'plowed' aside by the diamond stylus, is left in piles by the irregular lateral stylus movement.

To test both the reproducibility of these results and their sensitivity to surface oxidation, we carried out the series of measurements summarized in figure 8. The following procedure was used. First the threshold fields of a number of freshly made mechanical defects on a sample are measured. The sample is then removed from the SEM chamber and exposed for 2 h to the ambient air. It is then re-inserted into the SEM and the threshold fields are re-measured. For Au substrates (figure 8(*a*)), good reproducibility can be seen. For Nb substrates (figure 8(*b*)), there is increased scatter, reflecting the

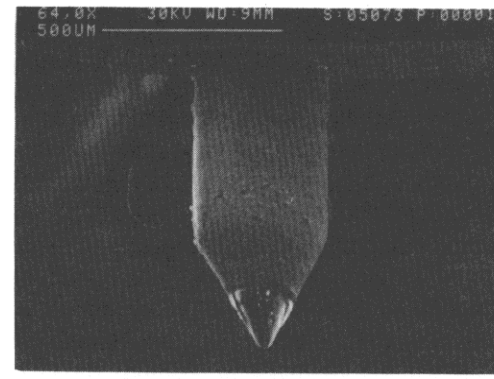

Figure 4. Mounting of diamond stylus used to create mechanical damage sites.

stronger instabilities observed in the emission current. In addition, there is a clear tendency toward higher threshold fields after air exposure. We suggest that this tendency is due to the restoration of the Nb oxide layer that was locally broken when the defect was created.

Figure 9 shows an example of a Fowler–Nordheim plot of the emission from a point defect, showing relatively good reproducibility on increasing and decreasing the applied field. For those mechanical damage sites with sufficiently stable emission to allow reproducible Fowler–Nordheim plots, the distribution of derived enhancement factors β and effective emitting

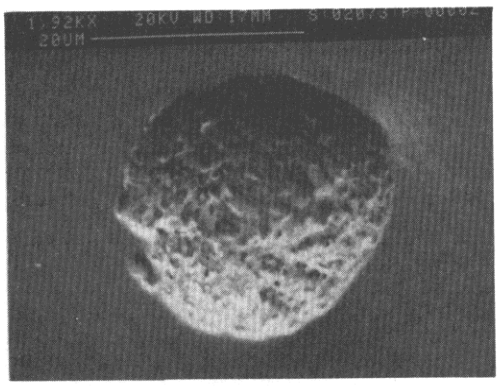

Figure 5. 'Point' mechanical damage site.

(*a*)

(*b*)

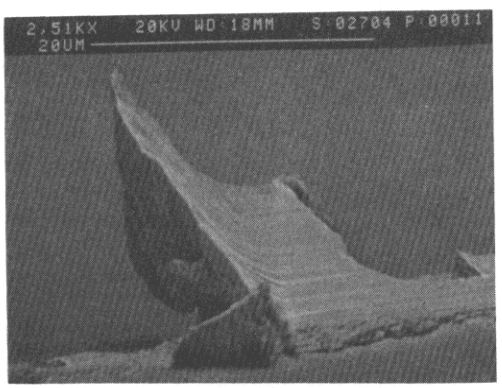

Figure 6. 'Scratch' mechanical damage site: (*a*) upper view, (*b*) lateral view.

areas S are shown in figures 10 and 11. These distributions are typical of those found in previous studies of naturally occurring emission sites [2].

Instability in emission current from a freshly created mechanical defect might be explained by the presence of a natural oxide layer or by the presence of a thin contamination layer resulting from our relatively poor vacuum (10^{-6} Torr). One would not expect a contaminant layer to depend strongly on the nature of the substrate, while oxide is formed on Nb and not on Au. As emission instabilities are more pronounced on Nb than on Au, we attribute them to oxidation. The presence of such a superficial layer also means that one must be cautious about applying the Fowler–Nordheim theory. Since this theory assumes a bare metal surface,

(*a*)

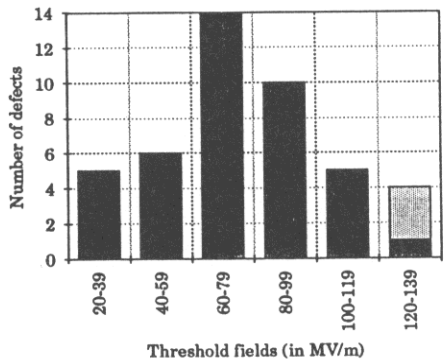

(*b*)

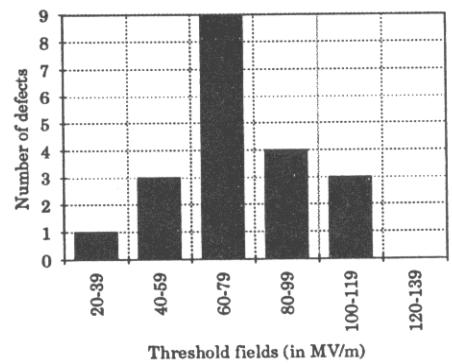

Figure 7. Emission tests for point mechanical damage sites. Dark bars show threshold fields for measured emission; light bars show maximum field attained when no emission was seen. (*a*) Point defects on a Nb substrate, (*b*) point defects on a Au substrate.

the area parameter S obtained from a Fowler–Nordheim fit to measurements on an oxidized surface can no longer necessarily be interpreted as the true emitting area.

One might argue that emission from a scratch could be due to some chemical contamination from the stylus. This hypothesis can probably be rejected, because scratch emitters can be produced by very different styli (for example diamond or tungsten), provided that they are hard enough to produce some mechanical damage on the cathode surface. Moreover, EDX analysis of the scratched surface never revealed the presence of foreign elements.

Contacts were also made with a plastic stylus. Owing to the difference of hardness between plastic and metal, no geometrical defects were produced on the Nb surface. Further, no emission was observed from these contacts despite a considerable contamination of the Nb substrate by plastic particles.

4. Electrostatic theory and numerical simulations

One of the main reasons for previous hesitations concerning the applicability of the projection model has been the implausibility of projections of sufficient sharpness. Theoretical calculations for simple projection

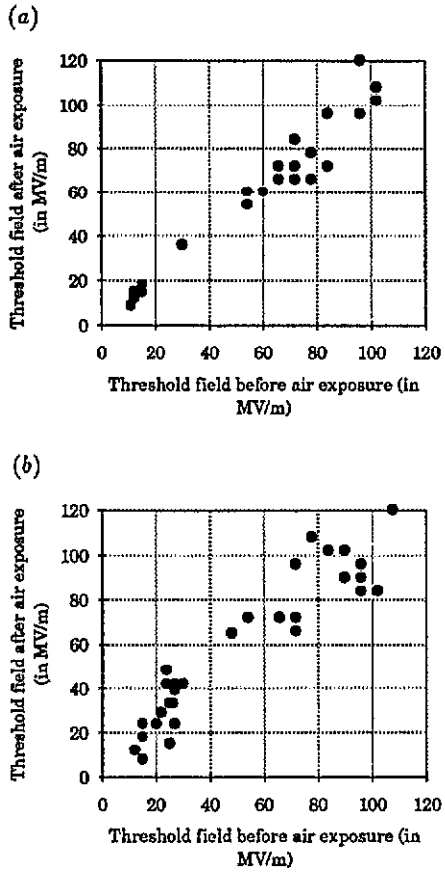

Figure 8. Effect of an air exposure on the threshold fields of point defects on a Au substrate (*a*) and on a Nb substrate (*b*).

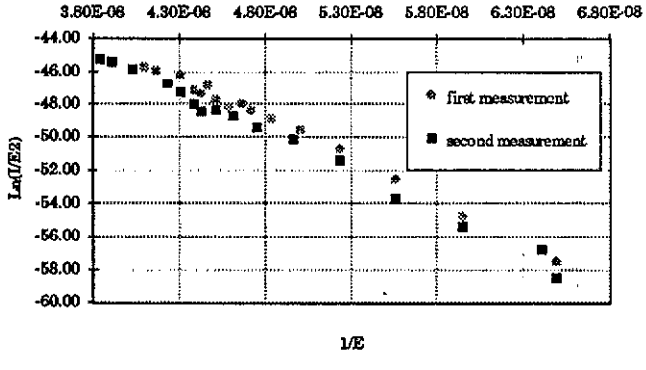

Figure 9. A Fowler–Nordheim plot of the emission from a point damage site on a Au substrate ($\beta_1 = 86$, $S_1 = 5 \times 10^{-10}$ m^2; $\beta_2 = 97$, $S_2 = 7 \times 10^{-11}$ m^2).

shapes (hemispheroids [11] and cylinders capped with hemispheres [12]) show that, roughly, the enhancement factor β is given by the ratio h/r, where h is the projection height and r is the radius of its tip. Thus the hemispherically capped cylinder (HCC) required to explain a β in the range 100–200, typical of those observed, would have to be some hundred times taller than its radius. No such projection is seen on either our irregular particles or on our mechanical damage sites, and the presence of such an acutely sharp feature on a scale too small to be resolved would seem quite implausible.

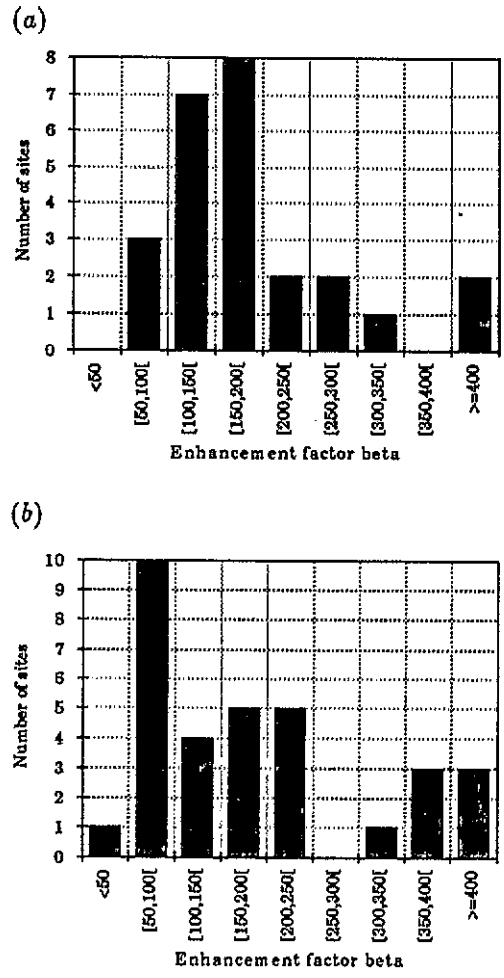

Figure 10. Enhancement factor β extracted from our current versus field values for mechanical damage sites on a Au substrate (*a*) and on a Nb substrate (*b*).

It seems not to have been noted in the literature, however, that there is a simple way to achieve a high β out of structures that are less sharp. Consider a HCC with sharpness sufficient to produce a field enhancement factor β_1. In a region sufficiently close to its tip, the projection surface will appear locally flat, with a uniform local field E_1 that is β_1 times greater than the field E_0 applied globally. A second, much smaller HCC with enhancement factor β_2 placed on this surface will itself experience a tip field E_2 enhanced over E_1 by a factor of β_2, or an overall enhancement $\beta = E_2/E_0 = \beta_1\beta_2$ (in the limit where the ratio of the sizes of the two HCCs goes to infinity).

To test this idea for finite values of h_1/h_2, we have carried out numerical calculations with the program POISSON [13]. This program solves Laplace's equation in two dimensions for specifiable geometry and boundary conditions using a relaxation method and a specifiable mesh; if cylindrical symmetry is assumed, then the calculation is effectively three- dimensional. Figure 12 shows equipotential lines calculated for two HCCs, each with $h_i/r_i = 8$ and thus [12] $\beta_i = 10$, for the case $h_1/h_2 = 5$. While calculation considerations limit the minimum usable mesh size, and thereby the size of the smallest geometrical feature that can be modelled, we have been able to carry out calculations, valid to about

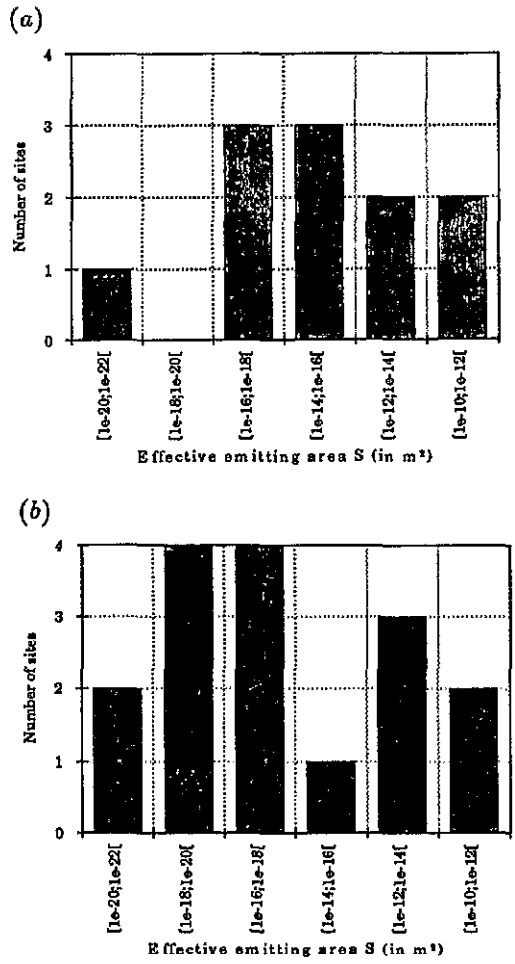

Figure 11. Effective emitting area S extracted from our current versus field values for mechanical damage sites on a Au substrate (*a*) and on a Nb substrate (*b*).

Table 1. Overall field enhancement factor β *calculated for a single hemispherically capped* projection, and for a superposition of two such projections with height ratio h_1/h_2, each with the same individual enhancement factor $\beta_i = 10$.

Projection	h_1/h_2	β
Single	—	10
Superposed	5	32
Superposed	10	50
Superposed	Infinite	100

$\pm 10\%$ inaccuracy, as far as $h_1/h_2 = 10$; the results are given in table 1.

5. Discussion

5.1. Particle geometry

In previous work [7], we have shown that the composition of a particle plays a role in its ability to emit. Here, we discuss two other parameters necessary to complete a global characterization of a particle's emission. These two parameters are the following.

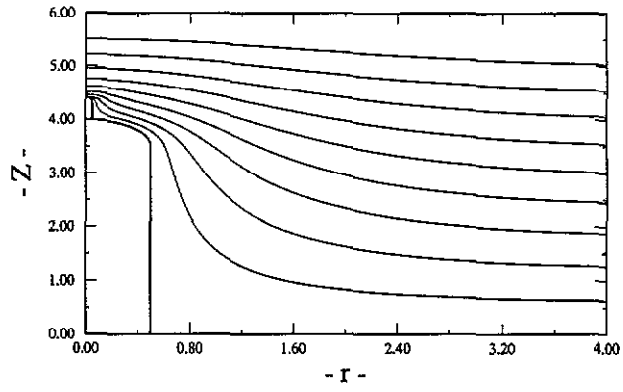

Figure 12. Calculated equipotentials for two superposed hemispherically capped cylindrical projections.

(i) Particle shape: no emission was seen from spherical particles of Ni or Fe for fields up to 120 MV m^{-1}. This lack of emission can be explained by the very small β of a sphere. In fact, a spherical particle gives a β of only 4, too small to produce measurable emission. That irregular particles emit is not surprising since we can easily expect these irregular particles to give larger and varying β values, in accord with the wide range of threshold values measured.

(ii) Interface between particle and substrate: field emission was observed from particles on an Au substrate with characteristics (threshold field, β values) quite similar to those measured for particles on natural or even anodized Nb substrates. This seems to indicate that the interface between particle and substrate does not play an important role (at least in the range of fields and currents with which we are concerned).

5.2. Damage sites

Once again, the method of creation of these sites, and their similarity on Nb and Au substrates, suggests only the possibility of projections. While our SEM does not allow us to resolve the fine details of the structures, it appears entirely plausible that a projection-on-a-projection model is consistent with both the observed geometry and the measured β and S values. In fact, β values of the order of 100 can readily be achieved with two superposed HCC structures of realistic dimensions, for example $h_1 = 10$ μm, $r_1 = 1$ μm, $h_2 = 100$ nm, $r_2 = 10$ nm. Such geometrical protrusions are within the range of observation of high-resolution scanning electron microscopes, and have indeed been observed on some geometrical defects produced by the above-mentioned method. A typical example is shown in figure 13.

5.3. Projection model

Many experimental findings seem to favour a 'geometrical' type of emission mechanism.

(i) In a previous paper [7], we found that insulating particles emitted much less than conducting ones.

(ii) It was shown above that spherical Ni and Fe particles do not emit, even for fields as large as

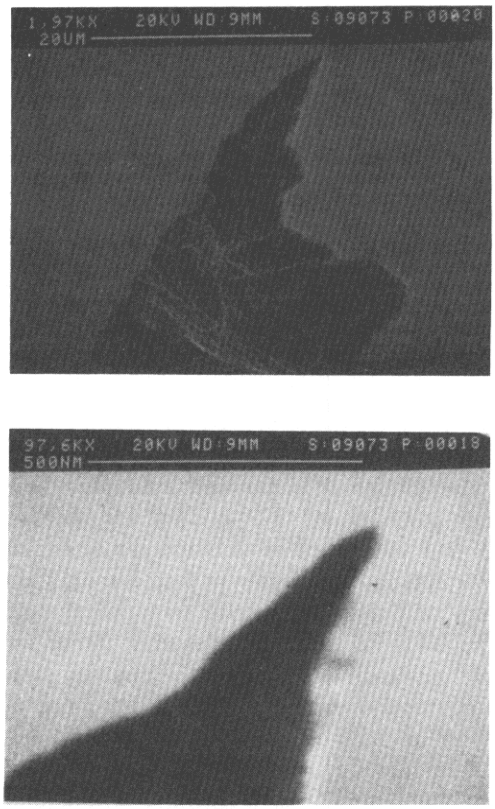

Figure 13. Geometrical defect with two superposed projections (threshold field 15 MV m^{-1}).

120 MV m^{-1}, whereas irregularly shaped particles of these metals strongly emit. The field enhancement factor for a perfect sphere is only 4, whereas the β expected from irregularly shaped particles is much higher. Morphological studies of the particle apex with the SEM did reveal very small radii of curvature at some places. In many instances, the observed radii were of the same order as the SEM resolution. It cannot be excluded that substructures exist on a still smaller scale, thus giving even larger β values.

(iii) The influence of an insulating layer separating a particle from the substrate seems to be small: the same emission behaviour was observed for similar particles on Nb and Au substrates.

(iv) After emission, it was often observed that conducting particles were in electrical contact with the substrate, even welded to it. Apparently the underlying oxide does not play an important role in the emission, since these welded particles continued to emit.

(v) Strong emission at low applied fields are observed on mechanical damage sites on a Au substrate.

(vi) The influence of an insulating layer on emission from mechanical damage sites seems to be small: the same behaviour was observed for sites on Nb and Au substrates.

All these features find a natural explanation if one admits that the particle or damage site behaves merely as a geometrical protrusion with a field enhancement at its apex. Our only result possibly at variance with this hypothesis involves the upper end of the range of effective area S extracted from our Fowler–Nordheim plots; values greater than 10^{-14} would seem difficult to reconcile with the assumption of a structure sufficiently small on the scale of our SEM's resolution. However, as suggested in section 3.2, the presence of a layer of oxide or other adsorbed species may influence sensitively the value extracted for S.

5.4. Conclusion

We have found strong evidence in favour of the projection model as an explanation for at least two kinds of emission sites (superficial metal particles and regions of mechanical damage), and we have weakened one of the traditional objections to this model. In fact, the hypothesis of superposed geometrical protrusions may well serve quantitatively to explain the enhanced field emission behaviour of the several types of sites that we have studied.

We do not wish, however, to go so far as to claim that all anomalous electron emission comes from projections. The measurements of electron and luminescent spectra referred to in the introduction continue to indicate that the naturally occurring sites examined in that research need a more complex model for their explanation. Naturally occurring sites studied by others [14] may indeed be of this type. We do claim, however, that both superficial metallic particles (such as Fe or Ag) and mechanical damage sites are potentially strong sources of electron emission that are much to be avoided in practical applications, and that the behaviour of this emission can be explained by the projection model.

Acknowledgments

We thank the Laboratoire de Métallurgie of the Institut National de Science et Techniques Nucléaires, Saclay, for allowing us the use of their SEM, without which we could not have carried out this work. We are also grateful to the other members of the group GECS for many helpful discussions.

References

[1] Latham R V 1981 *High Voltage Insulation: The Physical Basis* (London: Academic)
[2] Noer R J 1982 *Appl. Phys.* A **28** 1
[3] Fowler R H and Nordheim L 1928 *Proc. R. Soc.* A **119** 173
[4] Latham R V and Xu N S 1991 *Vacuum* **42** 1173
[5] Bayliss K H and Latham R V 1985 *Vacuum* **35** 211
[6] Hurley R E and Dooley P J 1977 *J. Phys. D: Appl. Phys.* **10** L195
[7] Jimenez M, Noer R J, Jouve G, Antoine C, Jodet J and Bonin B 1993 *J. Phys. D: Appl. Phys.* **26** 1503
[8] Tench D M and Yeager E 1973 *J. Electrochem. Soc.* **120** 164
[9] MacDougal B and Cohen M 1977 *J. Electrochem. Soc.* **124** 1185

[10] Wagner F T and Moylan T E 1989 *J. Electrochem. Soc.* **136** 2498
[11] Alpert D, Lee D A, Lyman E M and Tomaschke H E 1964 *J. Vac. Sci. Technol.* **1** 35
[12] Vibrans G 1964 *MIT Lincoln Lab Report 353*
[13] Accelerator Code Group, Los Alamos National Laboratory
[14] Niedermann Ph, Sankarraman N, Noer R J and Fischer Ø 1986 *J. Appl. Phys.* **59** 892